International Journal of Greenhouse Gas Control 110 (2021) 103396

Contents lists available at ScienceDirect

International Journal of Greenhouse Gas Control

journal homepage: www.elsevier.com/locate/ijggc

Opportunities for large-scale CO_2 disposal in coastal marine volcanic basins based on the geology of northeast Hawaii

Donald J. DePaolo [a,*], Donald M. Thomas [c], John N. Christensen [a], Shuo Zhang [d], Franklin M. Orr [b], Kate Maher [b], Sally M. Benson [b], Nicole Lautze [c], Ziqiu Xue [e], Saeko Mito [e]

[a] Energy Geosciences Division, Lawrence Berkeley National Laboratory, Berkeley, CA, 94720, USA
[b] School of Earth Energy and Environmental Science, Stanford University, Stanford, CA, 94305, USA
[c] Hawaii Institute of Geophysics and Planetology, University of Hawaii, Honolulu, HI, 96822, USA
[d] Department of Hydraulic Engineering, Tsinghua University, Beijing, 100084, China
[e] Research Institute of Innovative Technology for the Earth (RITE), Kizugawadai 9-2, Kizugawa-shi, Kyoto 619-0292, Japan

ARTICLE INFO

Keywords:
Carbon sequestration
Carbon mineralization
Hawaii
Volcano structure
CO2 hydrate

ABSTRACT

This paper presents an initial evaluation and concept description of an approach to CO_2 storage where the reservoir rocks are volcanic terrains that have been built up from the seafloor and consist of several kilometers of stacked lava, pyroclastic, and volcano-sedimentary rocks, and where CO_2 could be injected in large quantities in the supercritical or liquid state. These coastal "Saline Volcanic Basins" (SVB) have massive volume, heterogeneous internal structure, and relatively low temperatures. SVB's occur in island arcs and so-called hot spots such as Hawaii and Iceland. In both settings, the volcanic formations are exceedingly thick, border the ocean, are below sea level, and are saturated with seawater at storage depths. Many SVB reservoirs are accessible with onshore wells within which intercalated high and low-permeability layers and low temperatures can keep supercritical CO_2 in a relatively high-density state and promote solution and capillary trapping, in addition to mineralization. Some regions of the subsurface may be at low enough temperature to allow for CO_2 hydrate formation as an additional trapping mechanism. Our initial assessment of storage potential focuses on the northeast portion of the island of Hawaii, where there is direct information about the subsurface volcanic stratigraphy and hydrology based on observations made during two scientific drilling projects that penetrated to 3.5 km with continuous coring. Initial analysis, including simulations of a 50 Megaton injection of supercritical CO_2, suggests that this region could be effective for permanent storage, and potentially for gigatons of CO_2.

1. Introduction

Most research and development on Geologic Carbon Storage (GCS) is focused on deep saline sedimentary formations, appropriately because short-term trapping is usually available if there are sufficiently extensive low-permeability seal formations (DOE, 2015). However, there is value in expanding options for carbon storage into other types of reservoir rocks. Storage capacity of saline sedimentary reservoirs may be somewhat smaller than initially estimated (e.g. Kearns et al., 2017), and because the primary trapping mechanism is structural and other trapping mechanisms are substantially slower (Benson and Cook, 2005), CO_2 can remain as a separate phase for hundreds to thousands of years, which causes concerns about long term security and may require extended monitoring (Pawar et al., 2016). In addition, many countries, such as India, Japan, and Indonesia, do not have the appropriate geology, but may nevertheless have need for large-scale storage. The future could also include negative emission technologies (NAS, 2018) that could eventually allow storage reservoir locations to be decoupled from large stationary sources. Exploring the storage potential of other types of geologic formations also provides opportunity to discover other paradigms for CO_2 disposal, beyond reliance on widespread, continuous seal formations (e.g. Blondes et al., 2019).

In this contribution we discuss the potential for large volume CO_2 disposal (gigaton scale) into deep saline volcanic formations associated with coastal regions on the flanks of extinct volcanic terranes that have been built up from the ocean floor and consist of several kilometers of stacked lava, pyroclastic, and volcano-sedimentary rocks. These coastal marine "saline volcanic basins" constitute a large potential carbon

* Corresponding author.
E-mail address: djdepaolo@lbl.gov (D.J. DePaolo).

https://doi.org/10.1016/j.ijggc.2021.103396
Received 31 March 2021; Received in revised form 26 June 2021; Accepted 27 June 2021
Available online 16 July 2021

storage resource that has not been much investigated. Basaltic lava formations, both terrestrial and submarine, have been proposed as possible storage reservoirs based largely on the premise that injected CO_2 can be rapidly mineralized, and small scale storage has been demonstrated (Mito et al., 2008; Matter et al., 2016;(Matter and Kelemen, 2009) , McGrail et al, 2006, 2011, 2017a,b; Gislason and Oelkers, 2014; Goldberg et al., 2008; (Goldberg, 2017; Goldberg et al., 2010) Schaef et al., 2010, 2011; Snaebjornsdottir et al., 2018(Snæbjörnsdóttir et al., 2020)(Takahashi et al., 2000)). However, some estimates of mineralization timescales at temperatures less than 75°C suggest that for large-scale injection (10's of megatons), hundreds of years may be necessary before a large proportion of injected CO_2 is mineralized (Zhang and DePaolo, 2017). During this time, structural, solution, and capillary trapping may not be adequate to ensure near-zero leakage back to the atmosphere. Rapid mineralization could be expected at high temperature, as in the CARBFIX-2 demonstration (Clark et al., 2020; Snaebjornsdottir et al., 2020), but the need for temperatures >250°C further restricts applicability. In low to-moderate temperature sub-seafloor basalt at water depth greater than 2700 m, Goldberg et al (2008) proposed that storage security could be provided by other trapping mechanisms such as negative buoyancy of CO_2 and hydrate formation in addition to mineralization. Marieni et al (2013) also analyzed the potential for gravitational trapping for sub-ocean storage.

Similarly, our concept of large coastal saline volcanic reservoirs does not rely only on rapid mineralization of basalts, and differs from ocean floor basalt storage in that in general the reservoirs can be accessed by onshore wells. These coastal basins offer the potential, because of their massive thickness, heterogeneous internal structure, and relatively low temperatures, to provide sufficient short-term structural trapping to allow mineralization, dissolution, and capillary trapping in combination to be effective in yielding permanent trapping. The cyclic eruptive history of such basins can result in highly permeable flow breccias intercalated with low permeability flow interiors, ash, and hyaloclastite layers that represent multiple barriers to vertical flow (Fig. 1). There are still many uncertainties, however, because subsurface characterization of these reservoirs is minimal in comparison to continental sedimentary basins.

Large volcanic basins occur in island chains, where the volcanoes have been built up from the ocean floor by volcanic activity over millions of years. This type of geology occurs in island arc geologic settings like Japan, Indonesia, and the Aleutian Islands, and in so-called hot spot volcanoes such as Hawaii and Iceland (Lockwood and Hazlett, 2010). These volcanic reservoirs are (1) exceedingly thick (6 to 20 km) and composed entirely of volcanic rock, (2) border the ocean and, at storage depths (>1 km), are saturated with seawater or more saline formation fluids, and (3) can be at relatively low temperature due to proximity to cold deep ocean water and slow circulation of that water through the formations (Figure 1). In the context of CO_2 storage, these reservoirs may be favourable because i) they are largely accessible with onshore wells, ii) the low temperatures will keep CO_2 in a relatively high-density liquid or supercritical form, iii) the heterogeneity may be advantageous for both structural and solution trapping, and iv) the reactive rocks will promote mineralization. Many regions of the subsurface are also of low enough temperature that CO_2 hydrates can form (Brewer et al., 1999; House et al., 2006; Goldberg et al., 2008; (Goldberg, 1999); Teng and Zhang, 2018); the hydrates may be stable enough to act as an additional trapping mechanism (Fig. 1).

Fig. 2.

Globally, there are many sites where the coastal regions of large volcanic edifices could be evaluated for CO_2 storage potential. We have direct information about the subsurface volcanic stratigraphy and hydrology for the northeast section of the Island of Hawaii based on observations made during two scientific drilling projects that penetrated as deep as 3.5 km (DePaolo et al., 1996; Stolper et al., 2009) with continuous coring. This region can serve as a test bed for evaluating storage efficiency using available information about the subsurface. For this report we have supplemented previous studies with additional geochemical measurements on subsurface fluids and preliminary reactive transport models to evaluate the likely fate of injected CO_2. Ultimately, more extensive down-hole measurements and tests are needed in exploratory wells to better evaluate hydrologic properties and storage potential (e.g. Wheat et al., 2020).

2. Geology and Hydrology of Northeast Hawaii

Much of the direct knowledge of subsurface structure on the northeastern margin of the Island of Hawaii is derived from the results of drilling and coring during the Hawaii Scientific Drilling Project, which was active from 1993 to 2007. However, more general aspects of the structure of Hawaiian volcanoes can be deduced from models of volcano growth that have been developed over the past 30–40 years based on observations made of the surficial geology and seismically –determined subsurface structure (Moore et al., 1987; DePaolo and Stolper, 1996; Lipman and Calvert, 2013; Watts and ten Brink, 1989). The models to

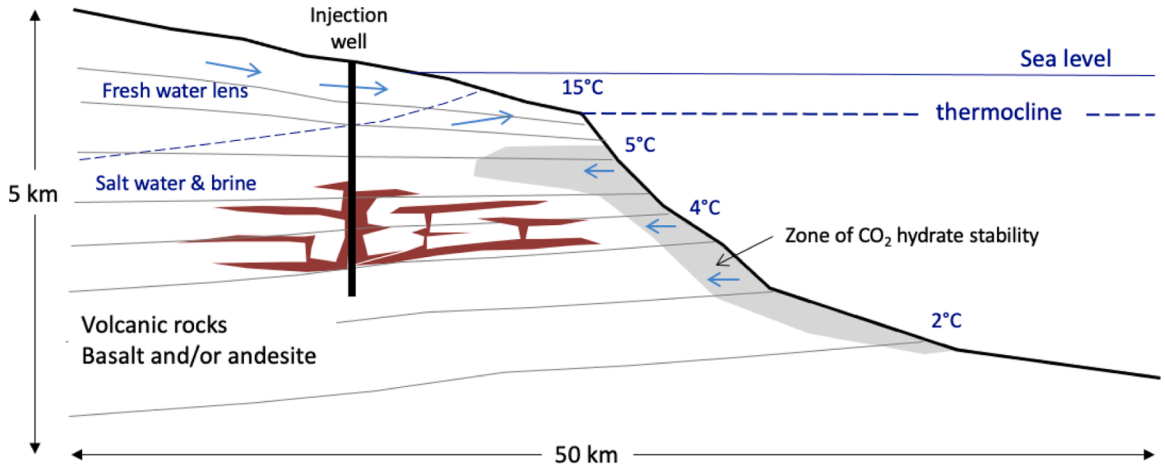

Fig. 1. General concept for large scale storage in near-shore saline volcanic basins, based on observations from northeast Hawaii and standard models for ocean temperature and fluid circulation in near-shore regions. Blue arrows show schematic fluid flow directions. Also shown is a conceptual sketch of the distribution of supercritical CO_2 injected at 2 to 3 km depth from an onshore well and penetrating 10+ km into the volcanic formations, mostly along a small number of high permeability zones near the injection horizon. Zone of hydrate stability, estimated to be 300 to 3000 m in thickness, would immobilize any injected CO_2 that approached the deep ocean and prevent it from reaching the ocean.

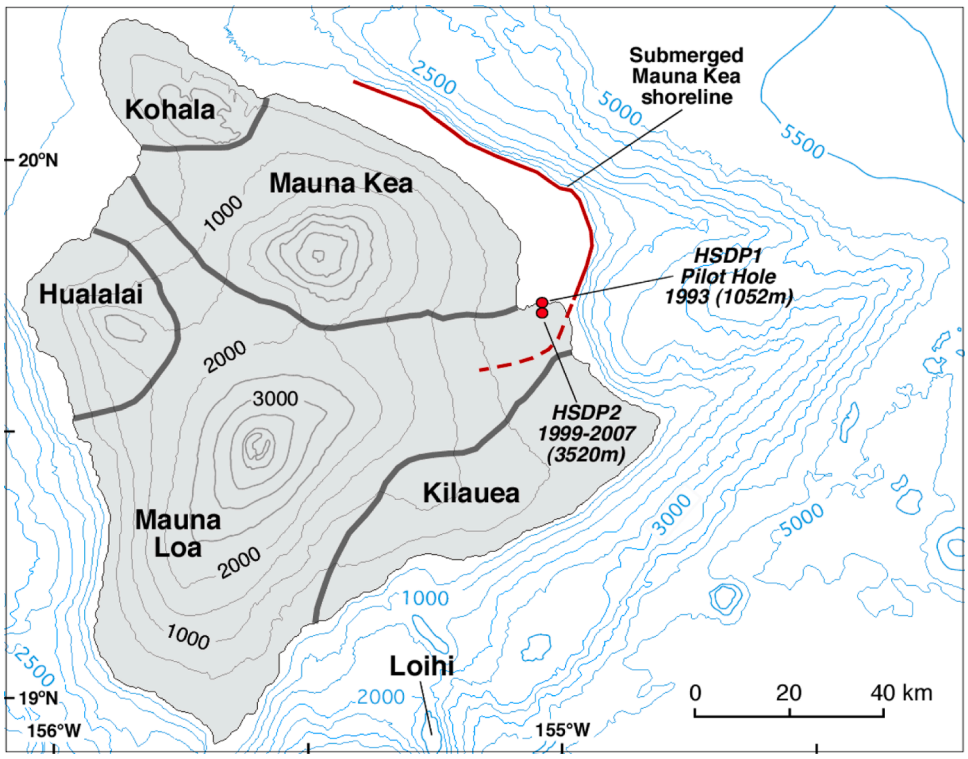

Fig. 2. Generalized topography and bathymetry of the island of Hawaii showing boundaries of the five volcanoes at the surface and the locations of the HSDP1 and HSDP2 boreholes (from Stolper et al., 2009). The red line shows the inferred location of the shoreline of Mauna Kea when the volcano reached its maximum size about 130,000 years ago. That shoreline has since subsided by 400 m or more as the crust under Mauna Loa and Kilauea volcanoes was loaded by continued volcano growth. Detailed bathymetry near the drill sites is provided in Fig. 9.

describe growth and subsidence of Hawaiian volcanoes are different in scale and mechanism from models for continental sedimentary basin evolution. For this reason, we describe some important aspects of Hawaiian volcano growth that lead to models for the internal structure of the volcanoes; models that we draw upon in evaluating CO_2 storage potential.

2.1. Geologic timescales

Continental sedimentary basins develop and evolve over tens of millions of years, and burial and diagenesis timescales can reach hundreds of millions of years. Hawaiian volcanoes grow over much shorter timescales. Estimated rates of vertical growth are 0.1 to 3 cm/yr (DePaolo and Stolper, 1996), about 100 times faster than continental sedimentation rates. A typical volcano is 12–16 km thick at its summit, so growth at 1.5 cm/yr implies that it takes about 1 million years to grow a single large volcano, an estimate that matches the time required for a volcano to drift over the top of a stationary hotspot magma source. The volcanoes are lozenge-shaped (Fig. 4), so the vertical thickness at the shoreline is about 6–7 km. Subsidence due to iso-static compensation, because it is relatively fast (order 10^4 years), can keep up with the growth of the volcanoes. By the time a Hawaiian volcano is fully grown, it has already subsided by about 5–7 km under the summit, and by 1–2 km at its shoreline (Fig. 3). After growth is complete, the volcanoes continue to subside, partly due to the plate motion moving them off of the mantle plume hot spot, and partly due to the continued growth of neighboring volcanoes further depressing the sea floor. The rocks under the HSDP drill sites extend in age from 1,800 years (youngest Mauna Loa flow) to about 650,000 years at 3500 m depth (Sharp et al., 1996; Sharp and Renne, 2004). Over the 650,000-year history, it is estimated that there has been about 1600 m of subsidence at an average rate of 2.5 mm/yr.

2.2. Internal structure and stratigraphy

The volcanoes of Hawaii are exceptionally large. The volume of a single Hawaiian volcano is about 30,000 to 60,000 km^3 (Lipman and Calvert, 2013; Robinson and Eakins, 2006). By comparison, typical stratovolcanoes, like Mt. Shasta in California or Mt. Fuji in Japan, are about 400 km^3; roughly 100 times smaller. The total volume of the island of Hawaii above the old ocean floor, comprising 6 volcanoes, is about 215,000 km^3 (Lipman and Calvert, 2013), which is similar to the volume of the Columbia River flood basalt province. The volume of the main series of Hawaiian islands (Hawaii through Kauai) is about 900,

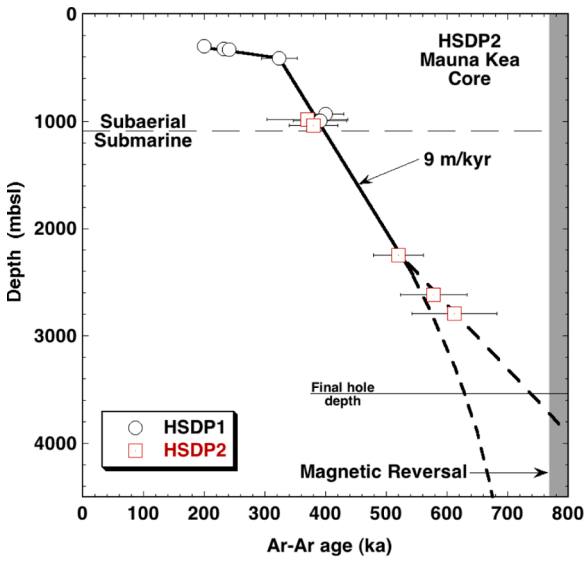

Fig. 3. ^{40}Ar-^{39}Ar ages of the rocks against depth. The subaerial alkalic basalt section at the top of the Mauna Kea sequence has a low accumulation rate (1 to 2 m/Ky) because it represents a waning phase of volcanic activity. Below that, the lava/hyaloclastite accumulation rate is about 9 m per thousand years. The rate is projected to get greater with depth. The oldest rocks sampled, at about 3500 m depth, are more than 650,000 years old.

000 km^3 based on an age of 6 Ma and an average eruption rate of 0.15 km^3/yr.

The internal structure of the volcanoes can be understood by considering how they form. Hawaiian volcanoes start as relatively small, steep-sided cones on the ocean floor that are made up mostly of pillow basalt as is the case for the currently active submarine volcano Loihi, and then grow to their final size over a period of about 1 million years (DePaolo and Stolper, 1996; Lipman and Calvert, 2013). About 20–25% of the way through the growth time, the volcano breaches the surface of the ocean. After this point in the growth the internal structure of the volcano is composed of three types of volcanic materials: pillow basalt, subaerially erupted lavas, and hyaloclastite (Figs. 4 and 5). The hyaloclastite forms as lava erupted at the volcano summit or from subaerial rift zones flows down to the shoreline and then is broken up and redistributed as volcanic sediment, forming a submarine deposit of glass-bearing clastic rocks around the volcano extending from the shoreline to the ocean floor in a steep-sided progradational apron that is about 15–20 km wide (Fig. 4).

2.2.1. Simplified volcano structure model

If the volcano were isolated and radially symmetric, and not as is actually the case with rift zones and overlapping older and contemporaneous volcanoes, a cross section would be expected to look like that in Fig. 4, which shows the three types of deposits in green (pillow lava), white with dashed lines (hyaloclastite), and brown (subaerial lavas). The diagram is drawn to represent the northeast part of Hawaii about 100,000 years ago, just after the Mauna Kea volcano reached its maximum area above sea level. The diagram also depicts subsidence of the ocean floor by about 6 km under the Mauna Kea summit, and about 1.5 km under the location of the drill site. Drilling results suggest this simple model is not accurate (see below), and that there is more pillow lava in the lower parts of the volcano near the shoreline. Other models suggest instead that dikes and other intrusive rocks occur much farther from the summit so that the region shown as hyaloclastite in this diagram is instead a mixture of pillow lava, hyaloclastite, and dikes and sills (e.g. Walker, 1987; Hill and Zucca, 1987). However, the HSDP drill core intersected very few dikes or other intrusives (Stolper et al., 2009). The proportion of hyaloclastite probably increases with (radial) distance from the summit (see Figure 6). In general, the subaerial slopes of Hawaiian volcanoes are relatively shallow (5–6°) and the submarine slopes are steeper (13–15°) (Mark and Moore, 1987).

The total subsidence under the volcanoes has been partially confirmed by seismic data (Hill and Zucca, 1987), but is largely based on models for loading and flexure of the oceanic lithosphere (Watts and tenBrink, 1989). The modern subsidence rate of 2.5 mm/yr at the drill site has been measured with tide gauges and this rate has been confirmed to apply over the past 400,000 years based on data from the HSDP drill core (Moore et al., 1996; Lipman and Moore, 1996; DePaolo et al., 1996). The HSDP-2 drill core passes through shoreline deposits at a depth of 1050 meters where the lavas have an age of about 420,000 years (Figs. 3 and 5). These observations confirm the long-term subsidence rate is close to 2.5 mm/yr.

2.2.2. HSDP2 core stratigraphy

The stratigraphy in the HSDP-2 borehole is different from the model shown in Fig. 4. In both models the upper 1000+ m is subaerial lava flows that have subsided below sea level. Below that, to a depth of about 2000 m, is a section made up mostly of hyaloclastite. However, instead of the hyaloclastite persisting uninterrupted all the way to great depth as in Fig. 4, the core below 2000 m returns to an interlayered sequence of pillow basalt and hyaloclastite that continues to the total depth drilled (3520 m). The depth to the old ocean floor is about 6.5 km based on subsidence models and seismic data (Watts and tenBrink, 1989; Hill and Zucca, 1987), so there is another 3 km of volcano below the maximum depth drilled for which we have no direct observations.

2.2.2. Modified volcano structure model

In light of the above discrepancies, our site model is modified (Fig. 6) to allow for more pillow basalt at depth. The reason for this structure is still conjectural, but it is consistent with what is known about volcano growth in general. The initial interpretation was that there was a volcanic rift zone located about 20 km north of the drill site and oriented east-west (see Fig. 8). However, the submarine feature that was identified as an extension of the rift zone has since been attributed to another volcano (Kohala), and the shallower bathymetry shows little indication of a large rift zone. A less extensive rift may have formed, but it must not have extended much beyond the modern shoreline location. The observations suggest that not all eruptions emanate from the summit, even if there is not a well-developed, long-lived rift zone. The cross section as shown in Fig. 6 is based on the inference that lava can be fed to distal parts of the volcano during its growth, but the frequency of off-summit eruptions decreases as the radius of the volcano increases. This leads to an increasing percentage of hyaloclastite with time and distance from the summit, and suggests that the lower part of the volcano is made up of a mixture of pillow lava, hyaloclastite, and probably also some intrusive rocks. The volume percentage of intrusive dikes and sills also decreases with distance from the summit. The amount of dike material intercepted in the HSDP borehole was small (a few % of the core) and much less than some earlier models had suggested (Walker, 1987).

2.3. Subsurface Temperature

An important characteristic of the NE flank of the island of Hawaii, and we suspect of many other near-shore marine volcanic regions, is low subsurface temperatures (Figs. 5 and 7). The depressed temperature is a result of cold deep seawater circulating through the flanks of the

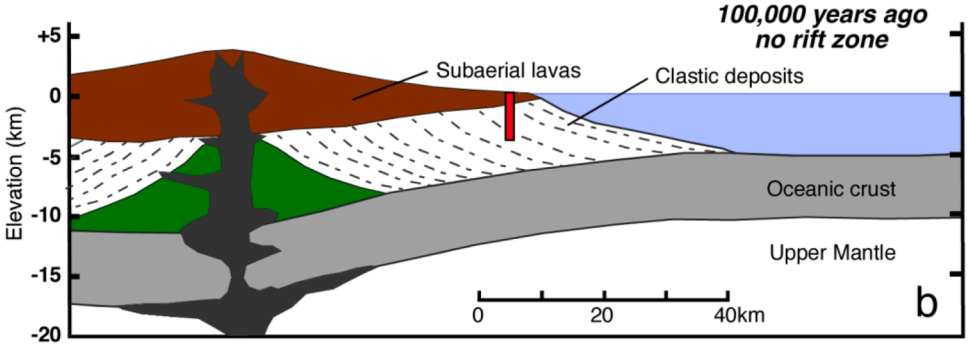

Fig. 4. Simplest model for the internal structure of Hawaiian volcanoes after the models of Moore and Chadwick (1995), taken from Stolper et al. (2009). The location and depth of the HSDP2 borehole is shown schematically in red. The volcano starts as a relatively steep-sided cone on the ocean floor, shown in green. After it breaches the ocean surface, sub-aerial lava flows erupting from the summit area flow down the slopes of the volcano to the shoreline where they break up and the fragments are redistributed down the steeper submarine slope to the ocean floor. The volcano shoreline then progrades out into the ocean as growth continues and the deeper flanks of the volcano are made up almost entirely of clastic material (which we refer to as "hyaloclastite," meaning clastic glass-bearing volcanic sediment). In this model, dikes and intrusions are found only directly under the summit.

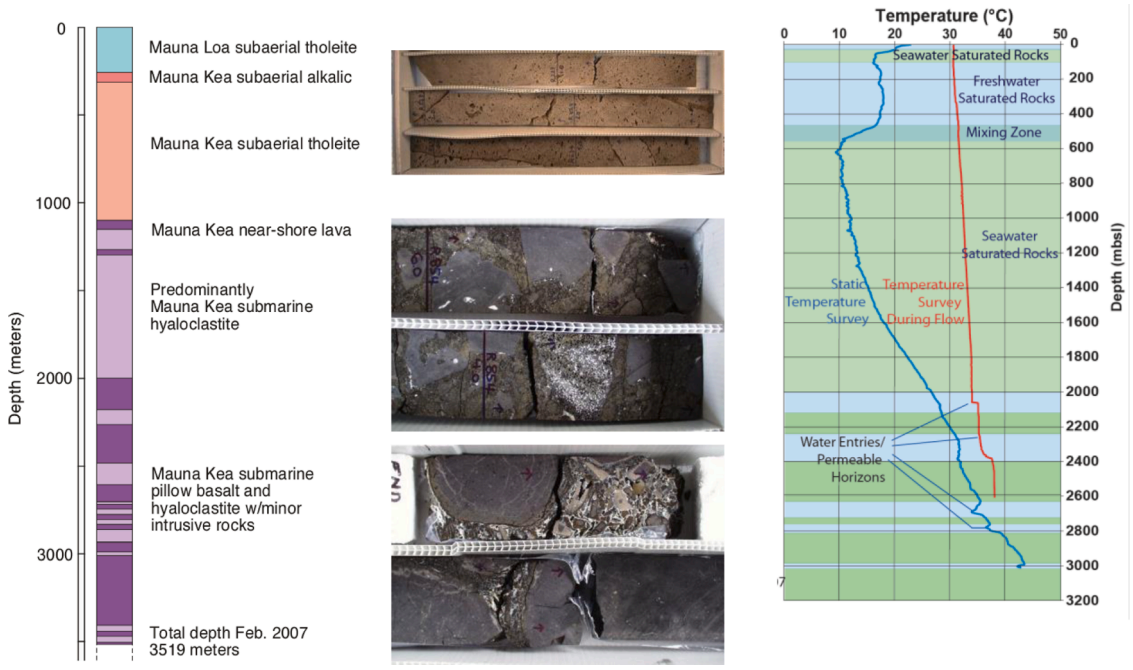

Fig. 5. (left) Summary of stratigraphy of the HSDP2 core. Subaerially emplaced lava flows from Mauna Loa and Mauna Kea extend from the surface to 1080 m depth. Below that level there is about 900 m that is mostly hyaloclastite. Below 2000 m the section is composed of interlayered pillow basalt and hyaloclastite. The most permeable layers are in sub-aerial basalt and the pillow lava sections. (middle) Examples of rocks cored from the three stratigraphic units. Mauna Kea sub-aerial a'a basalt at the top, hyaloclastite in the middle, pillow basalt at bottom. (right) Temperature measured in the HSDP2 well and the inferred relationships to subsurface hydrological features. Freshwater is shown as light blue, seawater as light green, and brackish waters as intermediate colors. Temperature survey (red line), done while the hole was flowing and still uncased below 1820 mbsl (meters below sea level), suggests that water was entering the hole below ~2800 mbsl, and additional entry levels are at 2370 and 2050 mbsl. Circulation of cold seawater through the section below 600 mbsl is rapid enough to cool the rocks by 25°C or more below a normal geothermal gradient. Figures adapted from Stolper et al. (2009).

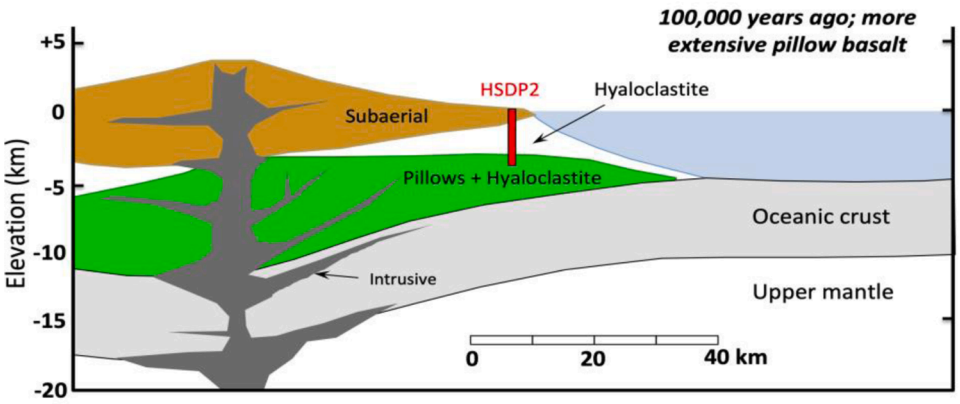

Fig. 6. Schematic internal structure of Mauna Kea volcano based on HSDP2 data and other studies (Stolper et al., 2009). This model forms the basis of our geologic site model as depicted in Fig. 9. The available data indicate that pillow lava can be emplaced far from the summit even in the absence of a large rift zone such as that making up the eastern arm of the currently-active Kilauea volcano. The implied structure indicates that the thickness of the hyaloclastite zone gets smaller in the direction toward the volcano summit and hence that the transition zone between the hyaloclastite and the underlying mixed pillow-hyaloclastite zone is likely to be a nearly horizontal, as well as gradational, surface.

volcanic pile at rates that are sufficiently fast to cool the rocks and depress the geotherm. There is an additional effect at the Hilo site because the lavas are young. As lava flows accumulate on the deep ocean floor, each one in turn cools to the ambient ocean temperature of 2–5°C. Consequently, the accumulating lava pile is generally at lower temperature than a steady-state geotherm would predict. The 6–7 km of lavas and other deposits at the Hilo site accumulated over about 750,000 years. The time required to reach thermal steady state by conduction for this thickness of rock is about 1 million years, so there is a lag in reaching steady state heat flow. In addition, the geothermal gradient in 80 million-year-old oceanic crust is quite low, about 15°C/km (Parsons and Sclater, 1977; McKenzie et al., 2005).

2.4. Hydrology

Some of the key observations relating to hydrology can be inferred from the temperature profile measured in the HSDP2 well (Fig. 7). In the uppermost part of the section, between 50 and 400 m, there is a fresh water aquifer at a nearly constant temperature of about 18°C. This aquifer is fed by the prodigious rain that falls on the windward slopes of Mauna Kea above and to the west-northwest of the drill sites. At the HSDP2 site some of this water is flowing in artesian aquifers that are beneath a confining layer at about 280 m depth near the boundary between Mauna Kea lava flows and younger flows from Mauna Loa. This boundary may be marked by a soil horizon with relatively low permeability, although in general vertical permeability in the basalts may be low.

Depressed temperatures are found throughout the entire 3500 m

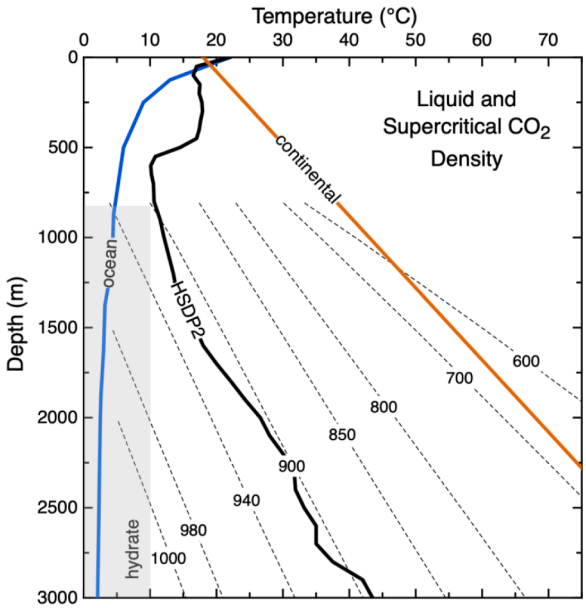

Fig. 7. Density contours of liquid and supercritical CO_2 and temperature-depth profiles for the HSDP2 borehole (Fig. 7), and for the ocean near Hawaii. A typical continental geotherm (25°C/km) is shown for comparison. The stability field of CO_2 hydrate is shaded. For the subsurface conditions between the HSDP2 well and the ocean, the density of CO_2 is between 900 and 1050 kg/m^3. Hydrostatic pressure is assumed for calculating the CO_2 density, which is based on the EOS of Span and Wagner (1996).

depth of the HSDP2 borehole. If a typical oceanic geotherm in 80 million-year-old lithosphere of roughly 15°C/km were present, starting with 24°C surface temperature, the temperature at 2000 m would be about 54°C and at 3000 m it would be 69°C. The measured temperatures are 27°C lower. Between 2000 and 3000 m depth, the gradient is in fact 15°C/km, which would suggest that fluid flow may not be strongly affecting the thermal gradient below 2000 m. However, hydrologic modeling done by Büttner and Huenges (2003) using a highly generalized model for the site suggests that there may be significant seawater inflow down to 6 km. The models suggest that seawater is being drawn into the section and is circulating in a clockwise direction when viewed from the south.

2.5. Geochemical constraints on subsurface flow

Geochemical measurements of fluids from the HSDP wells give some indication of likely flow rates. We have data on shallow fluids from the HSDP1 well, which is located at the shoreline about 2 km north of the HSDP2 site (Thomas et al., 1996). Fluids from the HSDP1 well at 600 to 800 m depth (Fig. 8) have temperature slightly lower than those at the same depth in the HSDP2 well, and similar to seawater at the same depth, indicating relatively rapid inflow. The fluid chemistry (salinity, Mg, Ca, SO_4, etc.) is also almost identical to seawater. If fluids are flowing along flow boundaries, then they probably originate from somewhat deeper levels of the ocean because of the 4 to 6° dip of the flows toward the ocean. The low temperatures in the HSDP1 well and the large depression of the geotherm above 1500 m depth in the HSDP2 well are indications of substantial fluid flow where cold ocean water is flowing through the rocks fast enough to remove geothermal heat. The radiocarbon age of fluid pumped from the HSDP1 well, which averages over the open interval between 720 m and 1050 m depth, is about 7200 years corrected for the radiocarbon age of seawater at equivalent depth (Thomas et al., 1996). It is estimated that the fluid would have traveled about 13 km to reach the site from the nearest seawater entry point on the subsurface slope of the volcano, suggesting a flow velocity of about 1.8 m/y, which may be an average of the faster flowing fluids above 800

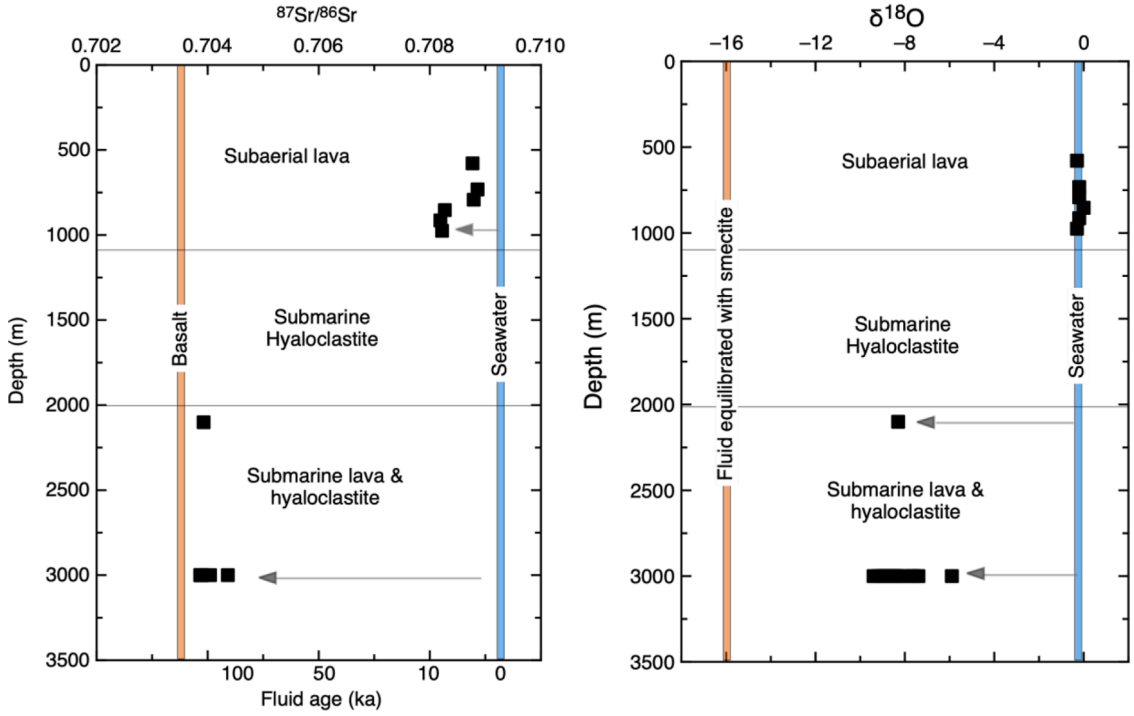

Fig. 8. Sr and O isotope data versus depth for fluids from HSDP1 and HSDP2 wells. Sr isotope ratios monitor dissolution of basalt minerals, which have $^{87}Sr/^{86}Sr \approx 0.7036$, much lower than the seawater value of 0.70918. Oxygen isotope effects are somewhat more complicated, but also reflected fluid-rock interaction as well as fluid source. The $\delta^{18}O$ of the samples from above 1000 m depth show that the fluids are seawater, and the Sr isotopes show they have reacted slightly with the rocks over a few to several thousand years (based on radiocarbon). Fluids pumped from the HSDP2 and derived from below the hyaloclastite layer show much more fluid-rock interaction and likely are much older. The age calculation is approximate for the deeper samples and explained in the text.

m and slower flowing fluids below 850 m.

Geochemical measurements can also provide some insight into fluid flow and basalt-fluid reaction rates. Strontium isotopes of dissolved Sr in fluids sampled from the 600 to 1000 m depth interval are shifted toward the values characteristic of the rocks ($^{87}Sr/^{86Sr} = 0.7036 \pm 0.0001$; Bryce et al., 2005), relative to the value for dissolved Sr in seawater ($^{87}Sr/^{86Sr} = 0.70918 \pm 0.00001$), which is constant and well-defined throughout the oceans (Kuznetsov et al., 2012). At 850–1000 m depth, the fluids are 3 to 4°C warmer than ocean water, implying that they may be flowing more slowly and have had more time to warm up than the fluids above 800 m depth. The larger shift in $^{87}Sr/^{86}Sr$ also indicates that they have been in contact with the basalt for a longer time period.

We can use the radiocarbon and Sr isotope results to derive an effective "Reaction Rate," which represents the fraction of the basalt that dissolves per unit time to contribute Sr to the fluid. The formulation for this rate (R) is:

$$\left(\frac{r_f - r_{sw}}{r_{bas} - r_{sw}}\right) = \left[1 - e^{-kt}\right]$$

Where $k = RfMK_{Sr}$ and $t = \frac{x}{v_f}$

The variables r_f, r_{SW} and r_{bas} are the $^{87}Sr/^{86}Sr$ ratios of the fluid sample, seawater and basalt respectively, M is the mass ratio of solid to fluid, $\rho_s(1-\phi)/\rho_f\phi$, and K_{Sr} is the ratio of Sr concentration in basalt (250 ppm) to seawater (8 ppm). The parameter f accounts for effects of fluid flow confined to fractures relative to a simple porous medium (DePaolo, 2006), x is the travel distance from the ocean to the borehole, and v_f is fluid velocity. From the well fluid measurements (average $^{87}Sr/^{86Sr} = 0.7086$ and age = 7200 years) we estimate a mean value for $RfMK_{Sr}$ of 1.5e-5 yr^{-1}. Using this average value, the fluid velocities for depths between 500 and 800 m are about 2.6 m/y and for depths of 850 to 1000 m the velocity is about 1 m/yr. Simple models of fluid circulation to account for the geotherm depression also suggest fluid velocities of meters/year.

In fluid samples extracted from HSDP2 well at depths below the base of the hyaloclastite layer, the $^{87}Sr/^{86}Sr$ is about 0.7039 (Fig. 8), which is much closer to the basalt value and indicative of much more extensive fluid-rock interaction. Other aspects of the fluid chemistry, including near zero Mg, high Ca, low Na, and $\delta^{18}O$ shifted to low values, also indicate extensive fluid-basalt interaction. The Cl content of these fluids is lower than that of seawater, so they may be mixtures of seawater and meteoric water. Using the same parameters and model deduced above, the estimated "reaction age" of the fluids would be 195 Ky. The equivalent velocity using 20 km for the travel distance would be 0.1 m/y. The estimate of age could be too high because the fluids are at higher temperature (30°C) and hence the reaction rate should be higher. However, these fluids have no detectable radiocarbon and hence must be older than about 30 Ka. If the age is bracketed by 30 and 100 Ka, it would correspond to fluid velocities of 0.2 to 0.7 m/yr assuming the fluid was sourced from the ocean (other work on similar area???). Hence the fluid velocities in the deeper parts of the section are substantially lower than in the upper 1000 m.

3. Geologic/hydrologic site model

Our site geological model is based on the data shown above in Figs. 3, 5, and 6, the bathymetry shown in Fig. 9, extensive geologic mapping of the volcanoes (Sherrod et al., 2007), and the temperature structure of the ocean around Hawaii. The subsurface structure and stratigraphy are summarized in Fig. 10. There are three major stratigraphic units (Fig. 5). The youngest and uppermost unit is composed of sub-aerial lava flows from the Mauna Kea (and Mauna Loa) volcanoes. This unit is about 1000 m thick at the HSDP2 drill site, tapers to near-zero thickness at the

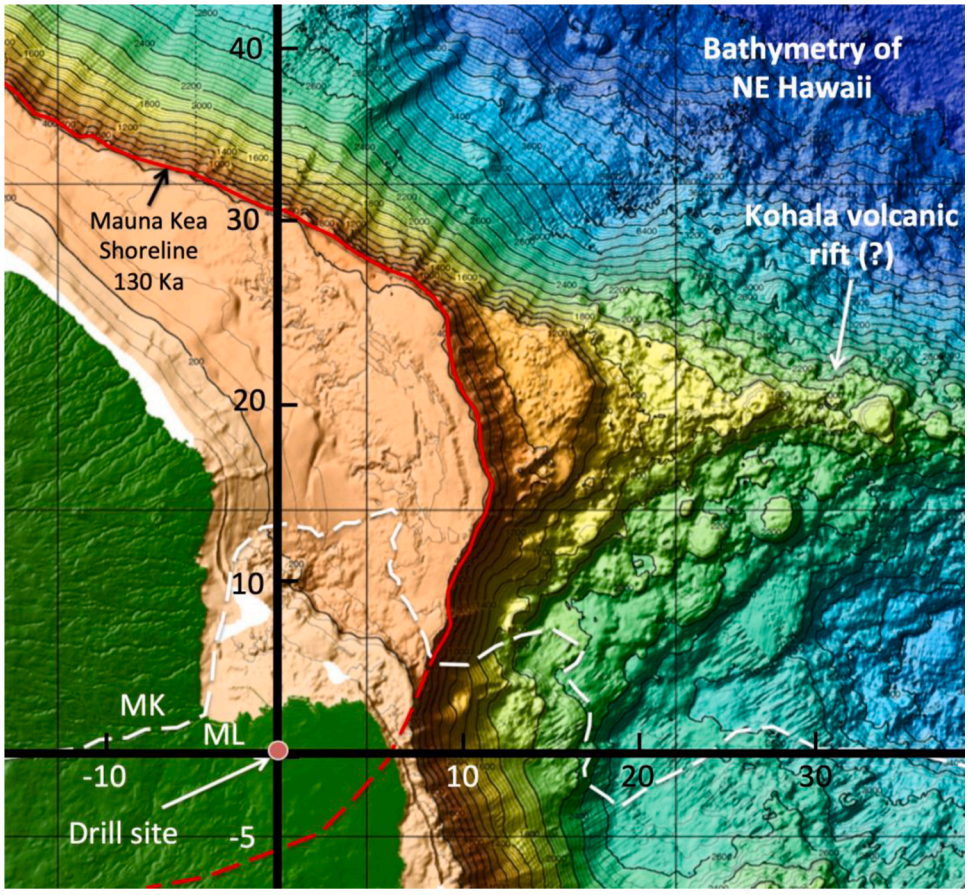

Fig. 9. Detailed bathymetric map of the study area. Land area shown in green. The black lines are the locations of the cross sections shown in Figs. 10a and 10b. The location of the paleo-shoreline of the Mauna Kea volcano at the time it started subsiding faster than it was growing is shown in red. Based on sea level history and the local subsidence rate, the age of that shoreline is about 130,000 years. The boundary between Mauna Kea (MK) and Mauna Loa (ML) lava flows exposed at the surface and on the ocean floor is shown in white. The submarine rift structure in the upper right side of the map has been interpreted as belonging to an older volcano (Kohala; Lipman and Calvert, 2011). Base map is from the Multibeam Bathymetry Data Synthesis, Chart 200-005, SOEST, University of Hawaii, Manoa.

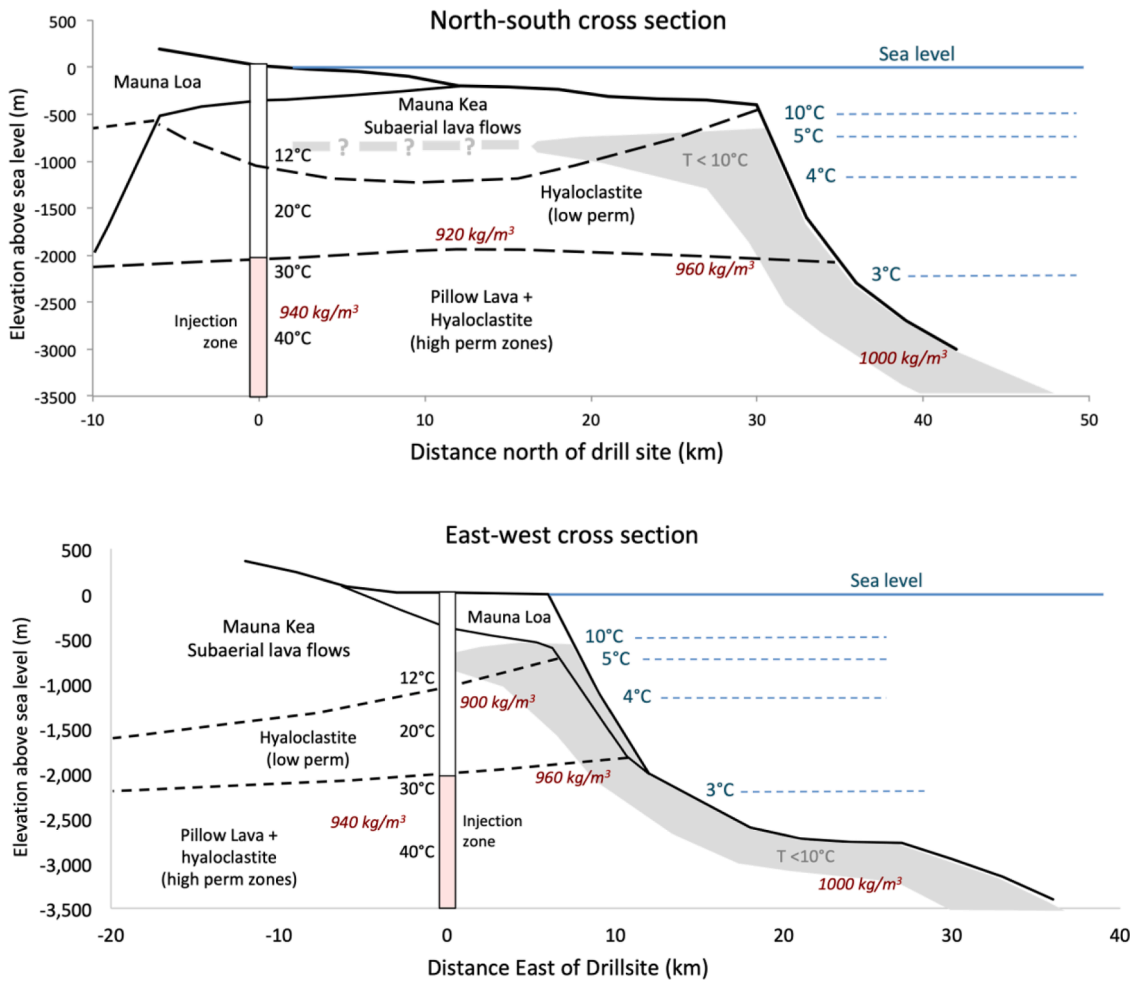

Fig. 10. (a) N-S cross-section and (b) east-west cross section of the eastern flank of the Mauna Kea volcano showing inferred boundaries of major lithologic units (subaerial lava flows, hyaloclastite, submarine pillow basalt) and location of existing HSDP2 drill hole. Vertical exaggeration is about 7x. Temperatures shown are measured in the borehole (shown in black type) and typical of central Pacific Ocean water (shown in blue type). The inferred density of liquid CO_2 is shown in red italic type at 4 locations in each cross section. The region where temperature is likely to be lower than 10°C so that CO_2-hydrate can form, is shaded; the thickness of this region is based on typical conductive temperature gradients. Note that a CO_2 injection of 50 million tons or less would be unlikely to flow into the formation more than about 2 km from the well (Fig. 11).

130 Ka paleo-shoreline, and thickens markedly to the west and northwest toward the summit of Mauna Kea.

The lavas composing the sub-aerial section dip 3° to 5°away from the Mauna Kea summit at the top of the section, and slightly more shallowly down section due to tilting associated with the large amount of subsidence to the west under the summits of Mauna Kea and Mauna Loa volcanoes. The age of the sub-aerial Mauna Kea lavas is between 200 and 400 Ka (Fig. 3). Below the sub-aerial lavas is about 1000 m of hyaloclastite, composed of indurated broken-up, glassy fragments of sub-aerial lava that flowed across the shoreline into the ocean. The contact between the sub-aerial basalt and the hyaloclastite layer is inferred to dip shallowly westward toward the summit of the volcano. The age of the hyaloclastite is mostly between 400 and 500 Ka (Fig. 3). Below the hyaloclastite is a zone of mixed pillow basalt and hyaloclastite that extends to undetermined depth, but possibly all the way to old ocean floor at about 6.5 km depth. The youngest of the pillow lavas is about 500 Ka; the age reaches about 600 Ka at 3 km depth (Fig. 3) and is expected to increase with the depth to about 750 Ka at 6.5 km depth.

4. CO_2 trapping mechanisms

To determine whether sites like the northeast flank of Hawaii would provide secure and long-term storage of injected CO_2, a number of key physical and chemical mechanisms of retention and trapping need to be considered. Multiple trapping mechanisms and multiple barriers to flow of CO_2 to the surface can be effective in sequestering CO_2, but the evaluation of overall storage security is more complicated in the absence of a confirmed high quality seal. In this section, we consider each of the mechanisms and discuss how they can be evaluated.

Seal and Seal Integrity. The low-permeability hyaloclastite layer from 1400 to 2000 m depth in the HSDP2 drillhole (see Figs. 4, 5, 8) may provide a good primary barrier to vertical flow. It is likely that this stratigraphy extends over a large area, as shown in Fig. 8. It is possible, of course, that fractures through the hyaloclastite could provide paths for vertical flow, but it is unlikely that single fracture paths would penetrate the entire thickness, and the absence of fluid entries into the well between 1400 m and 2000 m suggests that in the lower 2/3 of this section there are few, if any, open fractures.

A key question is whether vertical transport of CO_2 is more or less difficult to establish than lateral transport in the higher permeability zones below 2000 m. If the areal extent of high permeability zones is large, as suggested by the thermo-hydraulic modeling of Büttner and Huenges (2003), it will be difficult to raise the pressure much above that needed initially to inject the CO_2. In this case, lateral transport in the higher permeability zones will be favored during the injection period, followed by a period of relaxation of the injection pressure gradient

during which gravity-driven flow may play a bigger role (see simulations below). However, it is observed that there is pressurized brine in some of the intervals, and hence notwithstanding the Büttner and Huenges (2003) modeling results, there is still uncertainty about whether the high conductivity zones encountered in the well are connected to a broader network of conductive zones that will accept large amounts of injected CO_2. The observed dip of formations 4° to 15° away from the volcano summit may also act to limit the extent of lateral flow, and tend to make the flow be preferentially toward the volcano summit.

Flow Due to the Injection Pressure Gradient. Injection of CO_2 induces a pressure gradient that modifies the existing pressure gradients in the flow zone. The existing gradients are a combination of naturally occurring subsurface flow of fresh water down the flank of the volcano and thermohaline convection of seawater drawn in at low temperatures at the ocean floor that is heated and partially mixed with lower salinity waters. Age estimates for water samples taken from the HSDP1 well suggest that the flows above 1000 m depth are significant, but still slow compared to those likely to be created by injection. The flow in the deeper parts of the section, below the base of the hyaloclastite layer at about 2000 m depth, appears to be much slower and there is little evidence for any connection to the ocean.

Density-driven Gravity Segregation. At the depth and temperature range being considered, the density of CO_2 (900 to 940 kg/m^3) is only a little lower than that of seawater (~1030 kg/m^3). This density difference will drive vertical flow, although the buoyancy force is about 5 to 10 times smaller than in continental saline formations where temperatures are higher. When the reservoir height is small in relation to its length, density contrast is large, and vertical permeability is large, gravity forces are influential in generating a thin tongue of CO_2 at the base of the confining layer that caps the reservoir. This effect is represented by the gravity number (N_{gv}) being near unity or larger (Ide et al., 2007). However, for the conditions anticipated in the subsurface of NE Hawaii, gravity effects are much reduced ($N_{gv} \leq 0.01$), which means that during injection the CO_2 should spread out both vertically and horizontally within the reservoir, promoting dissolution, capillary, and mineralization trapping.

CO_2 Dissolution. Saturating seawater (or fresh water) with CO_2 increases its density by 1 to 2 percent. Such higher density fluid will develop at the base of a gravity tongue, and will drive an instability that creates vertical fingers of descending denser water (Riaz et al., 2006). Once the CO_2 is dissolved, there is no longer a driving force for upward transport of CO_2. For the conditions anticipated in the Hawaii subsurface where the development of gravity tongues is not favored, dissolution trapping can start during injection and be a substantial component of overall trapping. It is also, of course, the first step in promoting mineralization.

Capillary Trapping. As water invades a zone occupied by CO_2, a capillary instability at pore throats traps bubbles of CO_2 that are essentially immobile under the pressure gradients likely to exist in the formations being considered. Water invasion happens when CO_2 dissolution removes volume from the CO_2 plume or when subsequent water injection occurs. Capillary forces also play important roles in determining how vertical migration occurs, with heterogeneity that occurs at small scale acting to limit vertical flow and augment trapping (Krevor et al., 2011). Capillary trapping is reasonably well understood for non-reactive porous rocks like quartz-rich sandstone, but its efficacy in basalts, where the porosity structure is highly heterogeneous, is less well known.

Hydrate Formation. CO_2 hydrates are stable at depths below 1000 m and temperatures below about 10°C (Brewer et al., 1999). Offshore seawater temperatures northeast of Hawaii at these depths are 3° to 4°C, so there will be a zone within the volcanic edifice near the interface between the submerged flank of the volcano and the ocean where hydrates can form if CO_2 and water are in contact. The thickness of the low temperature zone can be estimated from likely thermal gradients. Since the typical geothermal gradient is 15 to 20°C/km, if the ocean temperature is 4°C, there can be a zone a few hundred meters thick that has T ≤ 10°C.

Hydrates have been demonstrated to form in low temperature marine settings where there is abundant water (e.g. Brewer et al., 1999). In narrow flow channels, the hydrate will block flow (Teng and Zhang, 2018). Whether it would do so in wide fractures or channels, if they exist, is less certain, but it is clear that hydrate formation will reduce permeability and restrict flow if lateral transport of CO_2 delivers it to zones near the sea floor. The rate of formation of hydrate, and the rate of any sub-sequent dissociation, are questions that need to be addressed to assess the trapping permanence of hydrate formation. Although models of marine methane hydrate de-stabilization due to ocean warming have been assessed (Reagan and Moridis, 2008; Moridis et al., 2008), there has to date been no modeling of CO_2 hydrate behavior within sedimentary or volcanic formations, especially with regard to the efficacy of hydrate formation as a trapping mechanism in the context of leakage of CO_2 from the seafloor. However, in the likely injection scenarios that we have considered, injected CO_2 is unlikely to reach the volcano-seawater interface (Fig. 11).

Mineralization. Basaltic rocks are considered excellent reservoir candidates for *in situ* mineralization of CO_2 because they contain an abundance of divalent cations in phases such as olivine ($(Mg,Fe)SiO_4$), pyroxene ($(Ca,Na)(Mg,Fe,Al)(Al,Si)_2O_6$), plagioclase ($CaAlSi_2O_8$) and volcanic glass (Oelkers et al., 2008; Gislason et al., 2010). The relatively slow kinetics of silicate mineral dissolution compared to carbonate precipitation, means that the dissolution of silicate phases is the rate-limiting step in the formation of carbonate minerals (Gislason et al., 2010). In natural analogues of carbon sequestration where CO_2-rich fluids have interacted with basaltic rocks, calcite is observed replacing primary minerals, such as plagioclase and pyroxene, and as pore filling (Thomas et al., 2016), confirming the potential for rapid mineralization of small amounts of injected CO2, for example at the Carbfix site in Iceland (Matter et al., 2016) and the Wallula site in Washington (McGrail et al., 2017a,b). Dissolution rates for basaltic minerals depend strongly on temperature, which varies significantly across the flow region, but is generally low in Hawaii (Fig. 10). However, the candidate reservoir rocks may have other characteristics that could accelerate mineralization.

Most experimental and modeling studies to date have focused on the primary minerals that comprise freshly erupted basalt (e.g. Zhang and DePaolo, 2017). However, depending on the temperature and fluid source, post-depositional circulation of fluids at temperatures <100°C can result in conversion of the primary basaltic minerals to zeolites, smectites and palagonite (Alt et al., 1998; Walton and Schiffman, 2003; Neuhoff et al., 2006). This mineral assemblage is more stable thermodynamically, but also characterized by much higher specific surface areas (e.g., ~1000 m^2/kg for smectite vs ~1 m^2/kg for pyroxene) resulting in increased cation exchange capacity. For example, experiments on altered vesicular basalt from ca. 300 ka lava flows in Iceland demonstrate substantial and immediate release of Ca (and Mg) via exchange with Na in the inlet fluid (Thomas, 2017). A similar effect has been documented for volcanic sediment from the Nagaoka experiment in Japan (Beckingham et al., 2016, 2017). The released Ca and Mg is then available to combine with dissolved inorganic carbon to produce carbonate minerals.

Hyaloclastite from the HSDP2 core shows evidence of alteration to palagonite, smectite and zeolite, as well as fracturing and reduction of porosity from ca. 40–45% to about 20–30% at depths of 1 to 1.3 km below sea level (Walton and Schiffman, 2003). Smectite is observed throughout the core, both lining the pores and as grain-replacing cements, and can be up to 32% of the rock within more highly altered zones, although those do not make up a large portion of the core. Zeolite mineralization (e.g., phillipsite and chabazite) is predominantly observed at depths below 1.4 km as fibrous masses and as spherulites in pores and fractures. The secondary minerals are likely to accelerate mineralization initially, but they probably don't control the total

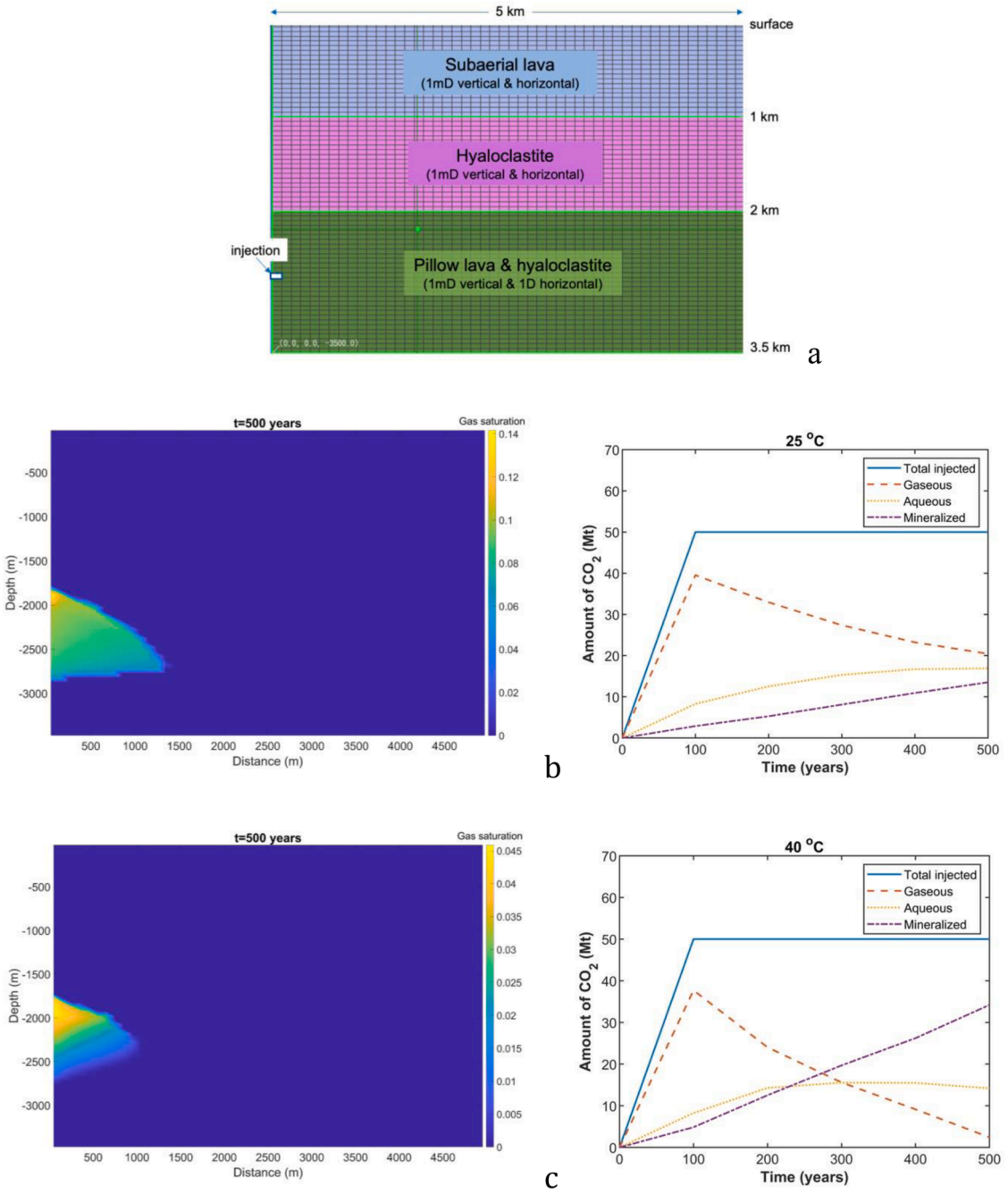

Fig. 11. Simulations at constant temperature of 25°C and 40°C using ToughReact. A total of 50 Megatons CO_2 is injected over 100 years. Injection overpressure is set to achieve that injection rate. Simplified basalt mineralogy is used (55% plagioclase; 25% clinopyroxene; 15% orthopyroxene; 3% magnetite, 1% quartz and 1% calcite). Reaction kinetics are from Palandri &Kharaka (2004) (labradorite and bronzite for the major minerals). Reactive surface areas for primary minerals are set to 2 m^2/kg.

amount of mineralization because of their relatively low overall abundance.

5. Injection models and trapping timescales

A key question is whether the combination of trapping mechanisms can provide a secure, multi-barrier setting for CO_2 storage in the long term. To begin to evaluate how the timescales for different trapping mechanisms relate, we have carried out simulations with TOUGHREACT software (Sonnenthal et al., 2014), using relatively simple assumptions regarding subsurface structure and hydrological properties. The simulations have so far been done only for an isothermal system and one where the formation boundaries have zero dip angle. Fig. 11a shows the lithologic structure and computational domain used and Figs. 11b and 11c show example results.

The model injection well is located at the left edge of the computational domain, and injection occurs from one grid block at a depth of 2.75 km. The geometry is a radially symmetric domain. Distance from the left boundary represents radial distance from the injection well. Supercritical CO_2 is injected at 0.5 Mt/yr for 100 years (50 Megatons total injected) and the simulation is run for a total of 500 years. Temperature is set at 25°C in one simulation and 40°C in the other. Other parameters are provided in the caption and figure. Büttner and Huenges (2003) deduced that the permeability of the pillow lava section below

the hyaloclastite was about 0.7 Darcy; we used 1 Darcy for the horizontal permeability. In the HSDP2 well the temperature at the base of the hyaloclastite layer is about 25°C and at the model injection depth of 2.75 km the temperature is about 37°C (Fig. 7. These isothermal simulations may bracket the behavior since they yield CO_2 of smaller and larger buoyancy relative to what would be expected along the HSDP2 temperature-depth curve (Fig. 7).

In both simulations the CO_2 does not rise much past the boundary with the main hyaloclastite layer at 2 km depth. Because the reservoir is unconfined the CO_2 spreads out in three dimensions, over a vertical distance of almost 1000 m, which enhances dissolution and ultimately, mineralization. At 25°C mineralization is relatively slow but the CO_2 density is high and it is less buoyant. At 40°C the CO_2 density is lower, but there is considerably more mineralization and after 500 years there is almost no remaining gas phase. As expected, based on the low gravity number, dissolution trapping starts immediately during injection and in both simulations 20 to 30% of the injected CO_2 is immobilized by dissolution.

In both scenarios, no CO_2 leaks from the system over 500 years, and none gets closer to the surface than 1.7 km. There would be more and faster reaction with some olivine and glass added, but since reaction rates are also determined by reactive surface areas and the rate laws used, both of which have considerable uncertainty, these calculations can be taken to suggest only that reaction *may* be fast enough to be significant on the time scale that CO_2 will be maintained in the subsurface by the limited vertical permeability, minimal buoyancy of the CO_2, and by dissolution trapping. Some kinetic formulations for pyroxene give rates 10 to 100 times higher than what we have used here, which would substantially accelerate mineralization if applicable. Reaction in the hyaloclastite also could be faster because of the high glass content, and it is possible this feature could make the hyaloclastite self-sealing. Reactions involving secondary minerals like palagonite and smectite are not considered in these simulations, but they are not expected to control the outcome because of their low overall abundance.

Although not especially fast at 25 to 40°C, mineralization begins immediately and continues at a near-constant rate for the duration of the simulation. Mineralization is significant mainly at some distance from the injection point (e.g. Zhang and DePaolo, 2017), because continued injection of CO_2 at high rates keeps pH low near the injection point, which initiates silicate mineral dissolution, but suppresses carbonate precipitation and growth. For this reason, rock-fluid interactions tend not to decrease permeability in the region near the injection point until after injection stops. Further modeling will use a dual-permeability formulation where fracture density and spacing can be adjusted. Previous modeling that considers vertical permeability heterogeneity in volcanic sedimentary rocks suggests that such heterogeneity enhances mineralization (Zhang et al., 2015).

Our conclusion from ToughReact modeling is that the geohydrology of the Northeast flank of the island of Hawaii could be an attractive locale for large scale CO_2 disposal because of the low subsurface temperatures and large volumes of reactive reservoir rocks. Low temperatures keep CO_2 dense and with minimal buoyancy. Lithologic heterogeneity, and in particular, the existence of a 1000 m-thick layer of glass-rich, low permeability hyaloclastite, are effective barriers to CO_2 escape over hundreds of years, a time period long enough to allow for extensive mineralization and dissolution trapping.

7. Application to other regions

An important question is the extent to which other locations in the world have geology that is similar enough to northeast Hawaii to have potential for large scale CO_2 disposal using the concepts discussed here. One area of immediate interest is the older Hawaiian Islands (Fig. 12). The internal structure of the Mauna Kea volcano that we have described is likely to apply to the other volcanoes in the chain. There may be variations due to varying growth rate or rift zone development that

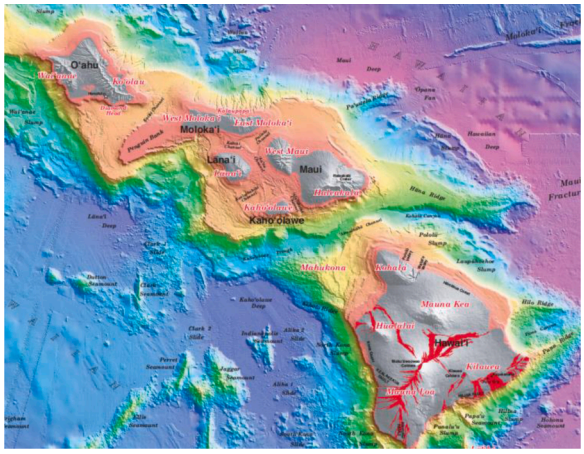

Fig. 12. Topographic – bathymetric shaded relief map of the younger Hawaiian Islands and surrounding seafloor (from Eakins et al., 2003). The target area for this project is shown as the light orange colored submarine terrace off the northeast coast of Hawaii. Other potential storage areas are the submarine terraces shown in light and darker shades of orange around Maui, Molokai, Lanai, Kahoolawe and Oahu. Much of this area can be accessed from onshore wells, but there may be additional large storage volumes that could be accessed with offshore drilling.

make the geology somewhat better or worse for this purpose. Also, the rocks that comprise older volcanoes may have lower permeability because they have undergone a longer history of diagenetic reactions. However, the amount of rock volume that could potentially be used for storage is large. The volume of the northeast flanks of the extinct volcanoes of the Island of Hawaii (Fig. 1) between 1 and 5 km below the surface and accessible with onshore drilling is roughly 10,000 km^3, of which about 10% is pore space. If 1–10% of this volume is effective storage volume, it is enough to hold 10-100 Gigatons CO_2. There may be an additional 100–200 Gigatons of capacity in the older islands from Maui to Oahu, especially if offshore drilling is included. These are rough numbers, but they suggest that the global capacity, including other analogous sites in Iceland and elsewhere, could be comparable to that estimated for deep saline formations. Similar large global capacity estimates for basalt have been discussed previously (Snaebjornsdottir et al., 2014; Goldberg et al., 2008), although those studies did not specifically evaluate the coastal marine settings we describe here.

Unlike the situation with the sedimentary basins of North America, there has not been extensive drilling and testing in the volcanic basins that might be favorable for CO_2 storage. Little is known about the subsurface permeability and porosity, and less yet about injectivity for CO_2. Even subsurface temperatures are uncertain, largely because seawater circulation and high rainfall severely impact the shallow temperature structure, making conventional heat flow measurements of little value (cf. Büttner and Huenges, 2003). In general, however, the geothermal gradient in old oceanic crust is low, and the proximity to cold ocean water and the circulation of some of that water through the volcanic pile, can markedly depress temperatures, making an environment where pure CO_2 has a density not much lower than formation water.

Other areas we think might be suitable for large scale storage using supercritical or liquid CO_2, in addition to intra-plate oceanic islands, are Iceland, Japan, the Aleutian Islands, and other island arc provinces like Indonesia. We do not have access to much relevant subsurface data from these regions. The northern island of Hokkaido appears to have some characteristics that might be favorable, as does the southern parts of Honshu. The mineralization potential for andesite may be somewhat less than that for basalt, but the proximity of these island arc rocks to large populations in Japan and Indonesia makes then an important target for future assessment.

8. Value of CO_2 disposal in oceanic islands

The value of having CO_2 disposal options in locations like Hawaii and Iceland goes beyond the potential for mitigating local emissions. Hawaii generates about 8 Megatons of CO_2 per year, not insignificant but only about 0.1% of global emissions. There is likely to be enough storage within the Hawaiian subsurface to accommodate all of the local emissions, but we have not evaluated the cost or techno-economic viability. If the rocks of the islands provide opportunities for secure disposal at a much larger scale it opens up other options relating to negative emissions technologies. One possibility is that local storage could allow for a low-CO_2, or even negative-emission approach to power generation in Hawaii. Currently power generation on Hawaii and similarly isolated islands is dominated by fossil fuel burning, and the fossil fuels must be imported to the islands. If, instead, Hawaii were to develop bioenergy as a source of electricity, and if the captured CO_2 could be disposed of locally on the islands, it could allow a high efficiency BECCS (Bio-Energy with Carbon Capture and Storage) approach to zero- or negative carbon power generation. There are likely to be abundant sources of biomass for combustion on the islands. One of the major hurdles for large scale BECCS deployment is co-location of sources and storage reservoirs (Baik et al., 2018), but this might be possible in Hawaii, because many of the likely high-capacity storage reservoirs are located on the windward side of the islands where the high rainfall would allow for rapid biomass production. A more complete assessment of the potential for large scale BECCS in Hawaii requires further investigation.

As atmospheric CO_2 concentrations climb and emissions also continue to increase, interest in other negative emissions technologies has increased (Keith et al., 2018; NAS, 2018; Energy Futures Initiative, 2019). If CO_2 can be captured directly from air (DAC; Direct Air Capture) then the primary issue is whether there are disposal options for the captured CO_2. Oceanic volcanic provinces have been considered previously in this regard (Goldberg et al., 2013) and currently there is a small component of DAC incorporated into the CO_2 disposal in Iceland (Gutknecht et al., 2018; Snaebjornsdottir et al., 2020). Another component of the problem is the provision of low-carbon energy to power DAC systems and storage activities. Oceanic islands like Hawaii have solar, wind, and geothermal energy production potential to help fill this power generation need, although additional evaluation of cost, land use, and infrastructure availability are required to determine feasibility.

9. Summary and conclusions

Analysis of available subsurface data for the northeastern part of the island of Hawaii, combined with models of volcano structure, analysis of available trapping mechanisms, and simulations of large-scale CO_2 injection, indicate that the flanks of large oceanic volcanoes provide opportunities for disposal of megaton-to-gigaton quantities of CO_2. Our analysis is based on the subsurface geology and hydrology of a region beneath Hilo, Hawaii, on the northeastern flank of the Mauna Kea volcano, where there is information available from previous NSF-sponsored scientific deep drilling projects (Hawaii Scientific Drilling Project or HSDP). The subsurface geology includes a thick layer of glass-rich clastic volcanic rocks at 1000 to 2000 m depth that may provide an effective seal. However, the volcanic stratigraphy in general may provide for effective permanent storage of large quantities of CO_2 due to the large reservoir volume, low vertical permeability, low temperatures that cause CO_2 to have high density and minimal buoyancy at projected storage conditions, and the tendency for effective solution trapping and mineralization. Preliminary injection models using TOUGHREACT and a simplified reservoir structure indicate that injection of 50 megatons of supercritical CO_2 over 100 years can be accommodated with zero leakage in the region near the HSDP borehole. Mineralization is substantial, but the overall paradigm is one where multiple trapping mechanisms can be used in concert to permanently sequester CO_2 in basalt.

Credit Author Statement

Donald J. DePaolo: Conceptualization, methodology, writing- original draft, supervision, visualization, project administration, funding acquisition

Donald M. Thomas: Methodology, Writing – review & editing

John N. Christensen: Investigation

Shuo Zhang: Investigation, methodology, software

Franklin M. Orr: Conceptualization, methodology, Writing – review & editing

Kate Maher: Conceptualization, methodology, Writing – review & editing

Sally M. Benson: Conceptualization, methodology, Writing – review & editing

Nicole Lautze: Writing – review & editing, project administration

Ziqiu Xue: funding acquisition, methodology, project administration

Saeko Mito: Investigation, methodology

Declaration of Competing Interest

The authors declare that they have no known competing financial interests or personal relationships that could have appeared to influence the work reported in this paper.

Acknowledgments

This research is supported by the Department of Energy, Office of Fossil Energy, under award number DE-AC02-05CH11231 to the Lawrence Berkeley National Laboratory. An insightful review by David Goldberg substantially improved the manuscript.

References

Alt, J.C., Teagle, D.A.H., Brewer, T., Shanks, W.C., Halliday, A., 1998. Alteration and mineralization of an oceanic forearc and the ophiolite-ocean crust analogy. J. Geophys. Res. Solid Earth 103 (B6), 12365–12380.

Baik, E., Sanchez, D.L., Turner, P.A., Mach, K.J., Field, C.B., Benson, S.M., 2018, Geospatial analysis of near-term potential for carbon-negative bioenergy in the Unites States. Proc. National Academy of Sciences 115, 3290–3295.

Beckingham, L.E., Mitnick, E.H., Zhang, S., Voltolini, M., Swift, A.M., Yang, L., Cole, D. R., Sheets, J.M., Steefel, C.I., Ajo-Franklin, J.B., DePaolo, D.J., Mito, S., Xue, Z., 2016. Evaluation of mineral reactive surface area estimates for prediction of reactivity of a multi-mineral sediment. Geochim. et Cosmochim. Acta v. 188, 310–329.

Beckingham, L.E., Steefel, C.I., Swift, A.M., Voltolini, M., Yang, Li, Anovitz, L.M., Sheets, J.M., Cole, D.R., Kneafsey, T.J., Mitnick, E.H., Zhang, Shuo, Landrot, G., Ajo-Franklin, J.B., DePaolo, D.J., Mito, Saeko, Xue, Ziqiu, 2017. Evaluation of accessible mineral surface areas for improved prediction of mineral reaction rates in porous media. Geochim. Cosmochim. Acta 205, 31–49.

Benson, SM, Cook, P., 2005. Underground Geological Storage. Carbon Dioxide Capture and Storage: Special Report of the Intergovernmental Panel on Climate Change (IPCC). Cambridge University Press, Interlachen, Switzerland, 5-1 to 5-134.

Blondes, M.S., Merrill, M.D., Anderson, S.T., and DeVera, C.A., 2019, Carbon dioxide mineralization feasibility in the United States: U.S. Geological Survey Scientific Investigations Report 2018–5079, 29 p., 10.3133/sir20185079.

Brewer, PG, Friederich, G, Peltzer, E, Orr Jr, FM, 1999. Direct experiments on the ocean disposal of fossil fuel CO2. ScienceScience 284, 943–945.

Büttner, G., Huenges, E., 2003. The heat transfer in the region of the Mauna Kea (Hawaii) – constraints from borehole temperature measurements and coupled thermo-hydraulic modeling. Tectonophysics 371, 32–40.

Clark, D.E. Oelkers, E.H., Gunnarsson, I., Sigfússon, B., Snæbjörnsdóttir, S.O., Aradóttir, E.S., Gíslason, S.R., 2020, CarbFix2: CO2 and H2S mineralization during 3.5 years of continuous injection into basaltic rocks at more than 250°C. Geochim. Cosmochim. Acta 279, 45–66.

DePaolo, D.J., 2006. Isotopic effects in fracture-dominated reactive fluid-rock systems. Geochim. et Cosmochim. Acta v 70, 1077–1096.

DePaolo, D.J., E.M. Stolper, D.M. Thomas, et al., 1996, The Hawaii Scientific Drilling project: summary of preliminary results: GSA Today, v. 6, no. 8, p. 1–8.

DOE, 2015. Department of Energy, Office of Fossil Energy, Carbon Utilization and Storage Atlas, 5th edition. The United States 2015.

Eakins, B.W., Robinson, J.E., Kanamatsu, T., Naka, J., Smith, J.R., Takahashi, E., Clague, D.A., 2003. Hawaii's volcanoes revealed. Geol. Investig. Ser. I-2809 1 (85), 342. U.S. Geological Survey, Washington, D.C.

Energy Futures Initiative (2019). Clearing the Air: A Federal RD&D initiative and management plan for carbon dioxide removal technologies. bit.ly/ClearingTheAirfullreport.

Gislason, S.R., Wolff-Boenisch, D., Stefansson, A., Oelkers, E.H., Gunnlaugsson, E., Sigurdardottir, H., Sigfusson, B., Broecker, W.S., Matter, J.M., Stute, M., Axelsson, G., Fridriksson, T., 2010. Mineral sequestration of carbon dioxide in basalt: a pre-injection overview of the Carbfix project. Int. J. Greenhouse Gas Control 4 (3), 537–545.

Gislason, S.R., and Oelkers, E.H., 2014, Carbon storage in basalt: Science, v. 344, no. 6182, p. 373–374. 10.1126/science.1250828.

Goldberg, D., 1999. CO2 sequestration beneath the seafloor: evaluating the in situ properties of natural hydrate-bearing sediments and oceanic basalt crust. Int J Soc Mater Eng 7, 11–16.

Goldberg, D.S., Takahashi, T., Slagle, A.L., 2008. Carbon dioxide sequestration in deep-sea basalt. Proceed. Natl. Acad. Sci. 105/29, 9920–9925. https://doi.org/10.1073/pnas.0804397105.

Goldberg, D.S., Kent, D.V., Olsen, P.E., 2010. Potential onshore and off-shore reservoirs for CO_2 sequestration in Central Atlantic magmatic province basalts. Proc. Natl. Acad. Sci. 107 (4), 1327–1332.

Goldberg, D.S., Lackner, K.S., Han, P., Slagle, A.L., Wang, Tao, 2013. Co-Location of Air Capture, Subseafloor CO_2 sequestration, and energy production on the Kerguelen Plateau. Environ. Sci. Technol. 47, 7521–7529.

Goldberg, D., 2017. Integrated Pre-Feasibility Study for CO_2 Geological Storage in the Cascadia Basin, offshore Washington State and British Columbia. National Energy Technology Laboratory. August.

Gutknecht, V., Snæbjörnsdóttir, S.Ó., Sigfússon, B., Aradóttir, E.S., Charles, L., 2018. Creating a carbon dioxide removal solution by combining rapid mineralizationof CO_2 with direct air capture. Energy Procedia 146, 129–134.

Hill, D.P., Zucca, J.J., 1987. Geophysical constraints on the structure of Kilauea and Mauna Loa volcanoes and some implications for seismo-magmatic processes. U.S. Geol. Surv. Prof. Pap. 1350, 903–917.

House, K, Schrag, D, Harvey, C, Lackner, K, 2006. Permanent carbon dioxide storage in deep-sea sediments. Proc Nat Acad Sci USA 103, 12291–12295.

Ide, S.T., Jessen, K., Orr Jr., F.M., 2007. Storage of CO_2 in saline aquifers: effects of gravity, viscous, and capillary forces on amount and timing of trapping. J. Greenhouse Gas Control 1, 481–491.

Kearns, J., Teletzke, G., Palmer, J., Thomann, H., Kheshgi, H., Yen-Heng, H.C., Paltsev, S., Herzog, H., 2017. Developing a consistent database for regional geologic CO_2 storage capacity worldwide. Energy Procedia 114, 4697–4709.

Keith, D.W., Holmes, G., St. Angelo, D., Heidel, K., 2018. A process for capturing CO_2 from the atmosphere. Joule v. 2, 1573–1594.

Krevor, SC., Pini, R., Li, B., Benson, S.M., 2011. Capillary heterogeneity trapping of CO_2 in a sandstone rock at reservoir conditions. Geophys. Res. Lett. 38 (15) https://doi.org/10.1029/2011GL048239.

Kuznetsov, A.B., Semikhatov, M.A., Gorokhov, I.M., 2012. The Sr isotope composition of the world ocean, marginal and inland seas: Implications for Sr isotope stratigraphy. In: Stratigraphy and Geological Correlation, 2012, 20. © Pleiades Publishing, Ltd., pp. 501–515, 2012.

Lipman, P.W. and Calvert, A.T., 2011, Early growth of Kohala volcano and formation of long Hawaiian rift zones: Geology, v. 39, p. 659–662.

Lipman, P.W., Calvert, A.T., 2013. Modeling volcano growth on the island of Hawaii: deep water perspectives. Geosphere v. 9. https://doi.org/10.1130/GES00935.1.

Lipman, P.W., Moore, J.G., 1996. Mauna Loa lava accumulation rates at the Hilo drill site: formation of lava deltas during a period of declining overall volcanic growth. J. Geophys. Res. v. 101, p. 11,631–11,641.

Lockwood, J.P., Hazlett, R.W., 2010. Volcanoes: Global Perspectives. Wiley-Blackwell, 536pp.

Marieni, C., Henstock, T.J., Teagle, D.A.H., 2013. Geological storage of CO_2 within the oceanic crust by gravitational trapping. Geophys. Res. Lett. 40 (23), 6219–6224.

Mark, R.K., and Moore, J.G., 1987, Slopes of the Hawaiian Ridge, in Decker, R.W., Wright, T.L., and Stauffer, P.H., eds., Volcanism in Hawaii: U.S. Geological Survey Professional Paper 1350, v. 1, p. 101–107.

Matter, J.M., Kelemen, P.B., 2009. Permanent storage of carbon dioxide in geological reservoirs by mineral carbonation. Nat. Geosci. 2, 837–841.

Matter, J.M., Stute, M., Snaebjornsdottir, S.O., Oelkers, E.H., Gislason, S.R., Aradottir, E. S., Sigfusson, B., Gunnarsson, I., Sigurdardottir, H., Gunnlaugsson, E., Axelsson, G., Alfredsson, H.A., Wolff-Boenisch, D., Mesfin, K., Taya, D.F.D., Hall, J., Dideriksen, K., Broecker, W.S., 2016. Rapid carbon mineralization for permanent disposal of anthropogenic carbon dioxide emissions. ScienceScience 352 (6291), 1312–1314.

McGrail, P.B., Schaef, H.T., Ho, A.M., Yi-Ju, Chien, Dooley, J.J., Davidson, C.L., 2006. Potential for carbon dioxide sequestration in flood basalts. J. Geophys. Res. v 111. https://doi.org/10.1029/2005JB004169.

McGrail, B.P., Spane, F.A., Sullivan, E.C., Bacon, D.H., Hund, G., 2011. The Wallula basalt sequestration pilot project. Energy Procedia 4, 5653–5660.

McGrail, B.P., Spane, F.A., Sullivan, E.C., Bacon, D.H., Hund, G., 2017a. Wallula Basalt Pilot Demonstration Project: post-injection results and conclusions. Energy Procedia 114, 5783–5790.

McGrail, B.P., Schaef, H.T., Spane, F.A., Cliff, J.B., Qafoku, O., Horner, J.A., Thompson, C.J., Owen, A.T., Sullivan, C.E., 2017b. Field validation of supercritical CO2 reactivity with basalts. Environ. Sci. Technol. Lett 4, 6–10.

Mito, S., Xue, Z., Ohsumi, T., 2008. Case study of geochemical reactions at the Nagaoka CO_2 injection site. Jpn. Int. J. Greenhouse Gas Control 2, 309–318.

McKenzie, D., Jackson, J., Priestly, K., 2005. Thermal structure of oceanic and continental lithosphere. Earth Planet. Sci. Lett. 233 (3-4), 337–349.

Moore, J.G., Ingram, B.L., Ludwig, K.R., Clague, D.A., 1996. Coral ages and island subsidence, Hilo drill hole. J. Geophys. Res. 101, 11,599-11,605.

Moore, J.G. and Chadwick, Jr. W.W., 1995, Offshore geology of Mauna Loa and adjacent areas, Hawaii. In Rhodes, J.M. and Lockwood, J.P. (eds) Mauna Loa Revealed: Structure, Composition, History, and Hazards, AGU, Washington, D.C., p. 21–44.

Moore, J.G., 1987, Subsidence of the Hawaiian Ridge, in Decker, R.W., et al., eds., Volcanism in Hawaii: U.S. Geological Survey Professional Paper 1350, v. 1, p. 85–100.

Moridis, G.J., Kowalsky, M.B., Pruess, K., 2008. TOUGH±HYDRATE v1.0 User's Manual: A Code for the Simulation of System Behavior in Hydrate-Bearing Geologic Media, Report LBNL-149E. Lawrence Berkeley National Laboratory, Berkeley, Calif.

NAS. National Academies of Sciences, Negative emissions technologies and reliable sequestration: a research agenda. 2018.

Neuhoff, P.S., Rogers, K.L., Stannius, L.S., Bird, D.K., Pedersen, A.K., 2006. Regional very low-grade metamorphism of basaltic lavas, Disko-Nuussuaq region, west Greenland. LithosLithos 92 (1-2), 33–54.

Oelkers, E.H., Gislason, S.R., Matter, J., 2008. Mineral carbonation of CO_2. Elements 4 (5), 333–337.

Palandri, J., Kharaka, Y., 2004. A compilation of rate parameters of water-mineral interaction kinetics for application to geochemical modeling. U.S. Geol. Surv. Open File Rep. 2004–1068.

Parsons, B., Sclater, J.G., 1977. An analysis of the variation of ocean floor bathymetry and heat flow with age. J. Geophys. Res. 82, 803–827.

Pawar, R.J., Bromhal, G.S., Chu, S., Dilmore, R.M., Oldenburg, C.M., Stauffer, P.H., Zhang, Y., Guthrie, G.D., 2016. The National Risk Assessment Partnership's integrated assessment model for carbon storage: A tool to support decision making amidst uncertainty. Int. J. Greenhouse Gas Control 52, 175–189.

Reagan, M.T., Moridis, G.J., 2008. Dynamic response of oceanic hydrate deposits to ocean temperature change. J. Geophys. Res. 113, C12023. https://doi.org/10.1029/2008JC004938.

Riaz, A., Hesse, M., Tchelepi, H., Orr Jr., F.M., 2006. Onset of convection in a gravitationally unstable, diffusive boundary layer in porous media. J. Fluid Mech 548, 87–111.

Robinson, J.E., Eakins, B.W., 2006. Calculated volumes of individual shield volcanoes at the young end of the Hawaiian Ridge. Volc. Geotherm. Res. 151, 309–317. https://doi.org/10.1016/j. jvolgeores.2005.07.033.

Schaef, H.T., McGrail, B.P., Owen, A.T., 2010. Carbonate mineralization of volcanic province basalts. Int. J. Greenhouse Gas Control v. 4 (2), 249–261.

Schaef, H.T., McGrail, B.P., Owen, A.T., 2011. Basalt reactivity variability with reservoir depth in supercritical CO_2 and aqueous phases. Energy Procedia v. 4, 4977–4984.

Sharp, W.D., Turrin, B.D., Renne, P.R., Lanphere, M.A., 1996. The 40Ar/39Ar and K/Ar dating of lavas from the Hilo 1-km core hole. Hawaii Scientific Drilling Project. Geophys. Res. 101, 11607–11616.

Sharp, W.D., Renne, P.R., 2004. The 40Ar/39Ar dating of core recovered by the Hawaii Scientific Drilling Project (phase 2), Hilo, Hawaii. Geochem. Geophys. Geosyst. 6 (4), Q04G17. https://doi.org/10.1029/2004GC000846.

Sherrod, D.R., Sinton, J.M., Watkins, S.E., and Brunt, K.M., 2007, Geologic Map of the State of Hawai`i: U.S. geological survey open-file report 2007-1089, 83 p.

Snæbjornsdottir, S.O., Wiese, F., Fridriksson, T., Armansson, H., Einarsson, G.M., Gislason, S.R., 2014. CO_2 storage potential of basaltic rocks in Iceland and the oceanic ridges. Energy Procedia 63, 4585–4600.

Snaebjornsdottir, S.O., Gislason, S.R., Galeczka, I.M., Oelkers, E.H., 2018. Reaction path modelling of in-situ mineralisation of CO_2 at the CARBFIX site at Hellisheidi, SW-Iceland. Geochim. Cosmochim. Acta 220, 348–366.

Snæbjörnsdóttir, S.Ó., Sigfússon, B., Marieni, C., et al., 2020. Carbon dioxide storage through mineral carbonation. Nat Rev Earth Environ 1, 90–102.

Sonnenthal, E. L., Spycher, N., Xu, T., Zheng, L., Miller, N., Pruess, K. (2014). TOUGHREACT V3.0-OMP.

Span, R., Wagner, W., 1996. A new equation of state for Carbon Dioxide covering the fluid region from the triple-point temperature to 1100 K at pressures up to 800 MPa. J. Phys. Chem. Ref. Data 25 (6), 1509–1596.

Stolper, E.M., DePaolo, D.J., Thomas, D.M., 2009. Deep drilling into a mantle plume volcano: the Hawaii Scientific drilling project. Sci. Drill. (7) https://doi.org/10.2204/iodp.sd.7.02. March 2009.

Takahashi, T, Goldberg, D, Mutter, JC, 2000. Secure, long-term sequestration of CO2 in deep saline aquifers associated with oceanic and continental basaltic rocks. In: Proceed- ings of the SRI International Symposium, Deep Sea & CO2 (The Ship Research Institute, Mitaka), 4-1-1–4-1-7.

Teng, Y., Zhang, D., 2018. Long-term viability of carbon sequestration in deep-sea sediments. Sci. Adv. 4, 3aao6588.

Thomas, D.M., Paillet, F., Conrad, M., 1996. Hydrogeology of the Hawaii Scientific Drilling Project borehole KP-1: 2. groundwater geochemistry and regional flow patterns. Geophys. Res. 101, 11683–11694. https://doi.org/10.1029/95JB03845.

Thomas, D., 2017. Geochemistry of CO_2 Sequestration in Basalts: Implications from Natural Analogues and Experimental Observations. PhD, Stanford University.

Thomas, D.L., Bird, D.K., Arnorsson, S., Maher, K., 2016. Geochemistry of CO_2-rich waters in iceland. Chem. Geol. 444, 158–179.

Walker, G.P.L., 1987, The dike complex of Koolau volcano, Oahu: internal structure of a Hawaiian rift zone, in Decker, R.W., Wright, T.L., and Stauffer, P.H., eds., Volcanism in Hawaii: U.S. Geological Survey Professional Paper 1350, v. 2, p. 961–993.

Walton, A.W., Schiffman, P., 2003. Alteration of hyaloclastites in the HSDP 2 phase 1 drill core - 1. Description and paragenesis. Geochem. Geophys. Geosyst. 4.

Watts, A.B., ten Brink, U.S., 1989. Crustal structure, flexure, and subsidence history of the Hawaiian Islands. J. Geophys. Res. 94 (10), 473–10,500.

Wheat, C.G., Becker, K., Villinger, H., Orcutt, B.N., Fournier, T., Hartwell, A., Paul, C., 2020. Subseafloor cross-hole tracer experiment reveals hydrologic properties, heterogeneities, and reactions in slow-spreading oceanic crust. Geochemistry,

Geophysics. Geosystems 21, e2019GC008804. https://doi.org/10.1029/2019GC008804.

Zhang, S,., DePaolo, D. J.; Voltolini, M. and Kneafsey, T. J., 2015, CO2 mineralization in volcanogenic sandstones: geochemical characterization of the Etchegoin formation, San Joaquin Basin, Greenhouse Gases: Science and Technology, v. 5, 622–644.

Zhang, S., DePaolo, D.J., 2017. Rates of CO_2 mineralization in geologic carbon storage. Acc. Chem. Res. 50, 2075–2084.